

Comparison of the Electron Momentum and Two-Photon Momentum Distributions in Titanium and Zirconium Dihydrides*

N.C. Bacalis

Theoretical and Physical Chemistry Institute, National Hellenic Research Foundation, Vas.
Constantinou 48, GR - 116 35 Athens, Greece

N.I. Papanicolaou

Physics Department, University of Ioannina P.O. Box 1186, GR - 451 10 Ioannina, Greece

D.A. Papaconstantopoulos

Naval Research Laboratory, Washington, D.C. 20375-5000, USA

We present first principles calculations of the electron momentum distribution and the two - photon momentum distribution of TiH_2 and ZrH_2 . These calculations are based on an augmented - plane - wave (APW) formalism and are used to understand differences in the band structure of the above hydrides. Predictions are made which will be very useful in the analysis of Compton scattering and positron annihilation experiments in the future.

Introduction

Metal - hydrogen systems have very interesting electronic properties and potential technological applications^{1/}. Among other experimental methods, Compton scattering^{2,3/} and positron annihilation techniques^{4/} have been successfully used for the determination of the electronic structure of metal hydrides. It is now well established that the ab initio band - structure calculations of the electron momentum density in these systems are necessary for the interpretation of various experimental results, like Compton profiles (CP) and angular correlation of positron annihilation radiation (ACPAR).

Recently we reported an augmented - plane - wave (APW) band - structure calculation of the electron momentum distributions (EMDs) and two photon momentum distributions (TPMDs) in Zr and ZrH_2 ^{5/} in order to understand the relation between the changes appearing in the momentum density upon the introduction of hydrogen and the changes of the respective energy bands. In the present work we report the calculation of the EMD and TPMD of TiH_2 using the same method and we compare with those of ZrH_2 mentioned above. The calculation was self - consistent (SC) and scalar - relativistic, within the local density formalism of Hedin - Lundqvist^{6/}.

Although Ti and Zr belong to the same group IV of transition metals, the band structures of their dihydrides differ mainly in the position of the level $\Gamma_{2'}$ with respect to the Fermi energy and the $\Gamma_{25'}$ level. These differences appear in the respective EMDs and TPMDs.

* Presented at the International Symposium on Metal - Hydrogen Systems, Fundamentals and Applications, Stuttgart, FRG, September 4 - 9, 1988.

Method of calculation

A detailed description of the calculational procedure is given elsewhere/5/. Here we report only an outline of the method. In the independent - particle model the TPMD is given by

$$\rho_{2\gamma}(\mathbf{p}) = \sum_{\mathbf{k}, j}^{\text{occupied}} \left| \int \exp(-i\mathbf{p}\cdot\mathbf{r}) \Psi_{\mathbf{k}, j}(\mathbf{r}) \Psi_{+}(\mathbf{r}) d^3r \right|^2$$

where \mathbf{p} is the total momentum of the emitted photon pair from positron - electron annihilations, $\Psi_{\mathbf{k}, j}(\mathbf{r})$ and $\Psi_{+}(\mathbf{r})$ are the wavefunctions of the electron in a state \mathbf{k} and in the j th energy band, and of the thermalized positron in its ground state $\mathbf{k}_{+} = \mathbf{0}$ respectively. The summation is over all one electron occupied states. The EMD $\rho(\mathbf{p})$ is given by the above expression, provided $\Psi_{+}(\mathbf{r})$ is set equal to unity.

The band - structure for both electrons and positrons in TiH_2 has been calculated self - consistently using the symmetrized APW method/7/. Darwin and mass - velocity relativistic corrections have been included, but spin - orbit coupling has been neglected. The exchange and correlation part of the electron crystal potential is treated in the local density approximation of Hedin and Lundqvist/6/.

TiH_2 and ZrH_2 crystallize in the cubic fluorite structure with lattice constants 8.3904 and 9.0329 a.u. respectively/5/.

Results and discussion

Electron Momentum Distribution

The calculated EMD $\rho(\mathbf{p})$ in TiH_2 is plotted in Fig. 1 (a) to (c), along the three symmetry directions [100], [110] and [111]. The relevant energy bands are shown in the insets. In Fig. 2 we show the EMD for ZrH_2 /5/. There are two main differences between the energy bands of TiH_2 and ZrH_2 : First the position of the $\Gamma_{2'}$ level (corresponding to hydrogen - hydrogen antibonding states) lies above the Fermi energy E_F in TiH_2 but below E_F in ZrH_2 . Second the same $\Gamma_{2'}$ state is above the d - like Ti states at $\Gamma_{25'}$ for TiH_2 , but below $\Gamma_{25'}$ for ZrH_2 . The first difference is, in SC calculations/8/, characteristic between the 3 - d and 4 - d metal dihydrides. The similarities and differences of the relevant energy bands in these two dihydrides appear in their momentum density.

According to selection rules/9/ only the bands Δ_1 , Σ_1 and Λ_1 contribute to the total $\rho(\mathbf{p})$ along the [100], [110] and [111] directions respectively, while the partial momentum density of other bands is zero along these directions. The labels (A), (B), etc., noted on the figures, are used to indicate the low and higher Δ_1 , Σ_1 and Λ_1 bands respectively. The lowest Δ_1 , Σ_1 and Λ_1 bands (labeled by A) are formed from metal - hydrogen bonding states/5/, where the contribution of the s - like H states is predominant. Hence the partial EMDs due to the above bands decrease slowly in the first Brillouin zone (BZ), and contribute with small values at higher momenta.

Along the [100] direction the next higher Δ_1 band (marked B in figures 1(a) and 2(a)) is partially occupied and has mainly a d - like metal character; for small \mathbf{p} its EMD behaves as p^4 . Therefore the Fermi break due to this Δ_1 band is not visible inside the first BZ, but in the region $1 < p < 2$ a.u., on either side of Γ , the two Fermi discontinuities, through Umklapp processes, are easily observable. The Fermi breaks for the two dihydrides occur at slightly different momenta, due to the different lattice constants.

As seen from Figures 1(b) and 2(b) the next Σ_1 band along the [110] direction (labeled by B), formed of essentially d - like metal character, is almost completely occupied and contributes to the total $\rho(\mathbf{p})$ with a smooth behavior. Thus along the [100] and [110] directions the EMDs of TiH_2 resemble those of ZrH_2 , because the respective energy bands contributing to the total EMD are of the same character, and the corresponding Fermi surface topologies are similar.

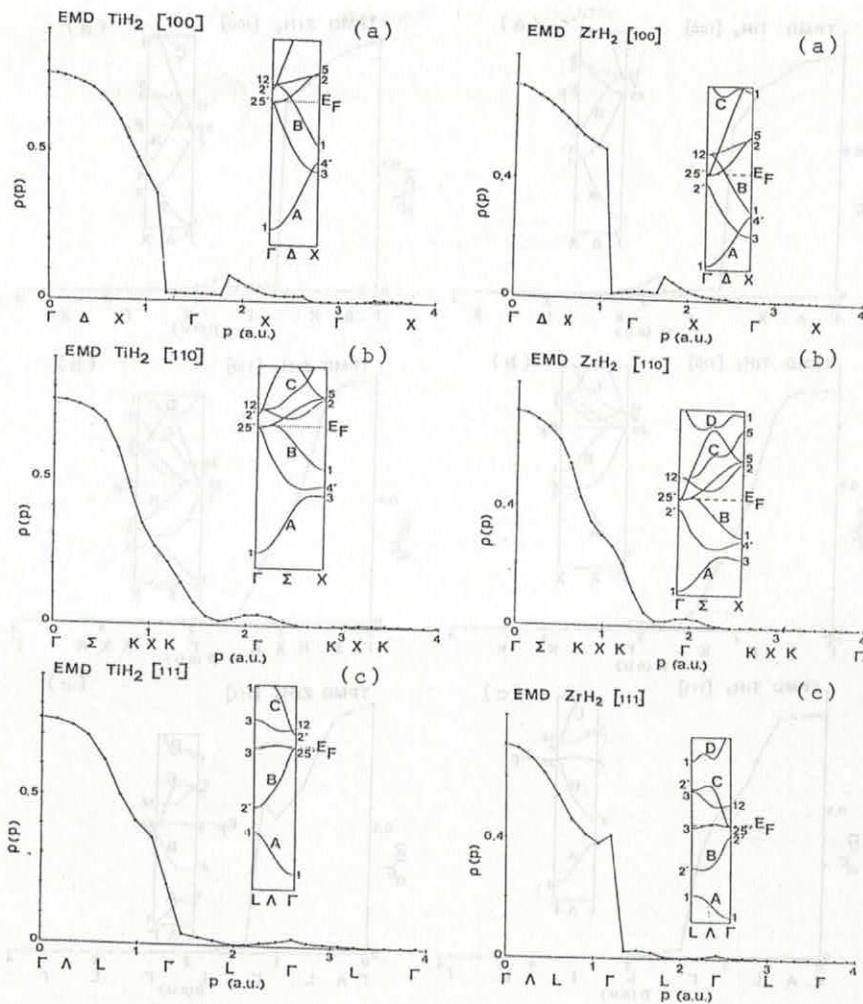


Fig. 1. Electron momentum distribution due to the band electrons of TiH_2 , along the [100] (a), [110] (b) and the [111] (c) directions. The solid lines connect the calculated points. The relevant energy bands are shown in the insets. The EMD is in arbitrary units.

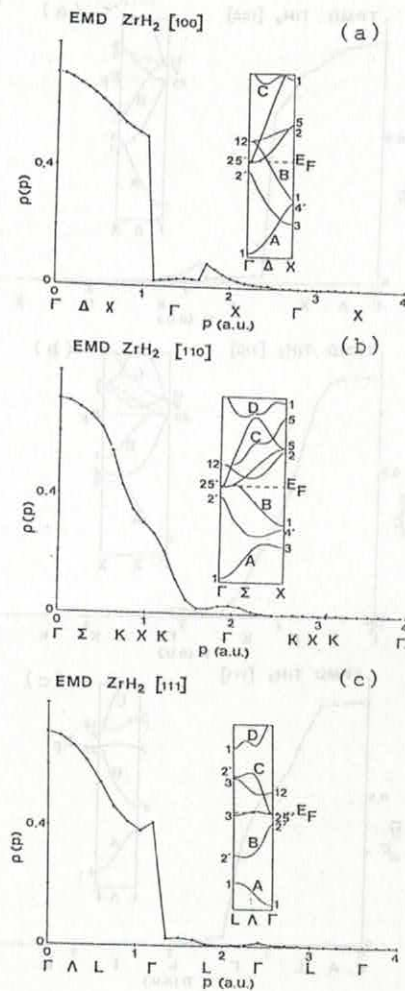


Fig. 2. The same as in Fig. 1, but for ZrH_2 .

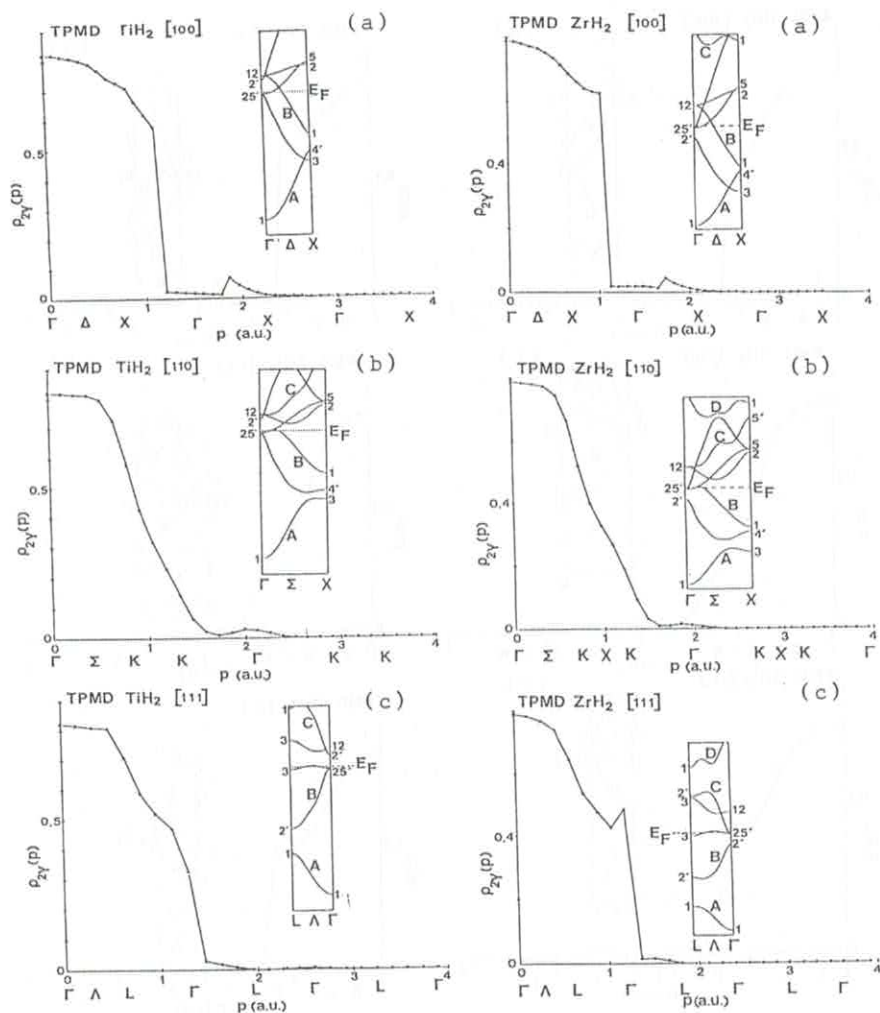


Fig. 3. Two-photon momentum distribution due to the band electrons of TiH_2 , along the [100] (a), [110] (b) and the [111] (c) directions. The solid lines connect the calculated points. The relevant energy bands are shown in the insets. The TPMD is in arbitrary units.

Fig. 4. The same as in Fig. 3, but for ZrH_2 .

Along the [111] direction however there is an essential difference: The second Λ_1 band of TiH_2 (marked as B in Fig. 1(c)), which is completely occupied, starts at $\Gamma_{25'}$ with a mainly d-like Ti character. So it fails to give a visible contribution at $p = 0$. When p increases the band hybridizes with mainly the hydrogen s-like states and also with other metal states, so its partial contribution to the total $\rho(\mathbf{p})$ increases and then decreases smoothly. Furthermore the next higher Λ_1 band (marked as C in Fig. 1(c)), which starts at $\Gamma_{2'}$, is unoccupied and does not contribute to $\rho(\mathbf{p})$. On the contrary in ZrH_2 , the second Λ_1 band (labeled by B in Fig. 2(c)) starts at $\Gamma_{2'}$ and not at $\Gamma_{25'}$ as in TiH_2 , and is completely occupied, while the next Λ_1 band (marked as C in Fig. 2(c)) starts at $\Gamma_{25'}$ and is only occupied near it. Thus a peak and a sharp Fermi break were observed in the [111] EMD of ZrH_2 (Fig. 2(c)) around $p = 1.2$ a.u. (near Γ) due to the partial contribution of $\Gamma_{25'}$ state/5/, which are now absent in the $\rho(\mathbf{p})$ of TiH_2 .

Two - photon momentum distribution

The theoretical total TPMDs $\rho_{2\gamma}(\mathbf{p})$ along the three symmetry directions [100], [110] and [111] for TiH_2 and for $\text{ZrH}_2/5/$ are shown in Figures 3 and 4 respectively. The high momentum components of the TPMD in TiH_2 have smaller amplitudes than those of the corresponding EMD, because of the presence of the positron wavefunction which decreases the contribution of core orbitals, being away from the nuclei. It is also shown from the figures 1(a) and 3(a) that the Fermi discontinuity on the TPMD of TiH_2 at $p = 1.2$ a.u. along the [100] direction is larger than that of the EMD, which is also true in $\text{ZrH}_2/5/$. Finally the respective TPMDs in TiH_2 and ZrH_2 (figures 3 and 4) have striking similarities along the [100] and [110] directions, and differences along the [111] direction, which can be explained in a manner similar to the one used for the EMDs.

Conclusions

We have presented EMDs and TPMDs in TiH_2 , calculated by a self-consistent APW method, and compared with those in $\text{ZrH}_2/5/$. The shapes of $\rho(\mathbf{p})$ and $\rho_{2\gamma}(\mathbf{p})$ along the [100], [110] and [111] directions are understood on the basis of the respective energy bands and the Fermi-surface topology. The differences of the momentum density between the two dihydrides, appearing mainly along the [111] direction, are explained in terms of the contributing energy bands near the Fermi energy, which differ in angular momentum character and Fermi-surface topology. It is well known/8/ that the above mentioned differences between the band-structures of the two dihydrides are generally characteristic only of SC calculations. Non-SC calculations of the energy bands of TiH_2 and $\text{ZrH}_2/10/$, give the same location of the $\Gamma_{2'}$ state with respect to E_F and the $\Gamma_{25'}$ state for both dihydrides. Compton scattering and positron annihilation experiments are needed to resolve this discrepancy.

We think that these results can be useful for analysing a future 3-dimensional reconstruction of $\rho(\mathbf{p})$ or $\rho_{2\gamma}(\mathbf{p})$ from directional CP measurements or ACPAR data, respectively. The experimental data would also check the existence of different momentum densities along the [111] direction in these dihydrides.

This calculation was performed at the Research Center of Crete.

References

1. Alefeld G. and Völkl J. (Eds.), Hydrogen in metals, vols. I and II, Berlin, Springer, 1978.
2. Williams B.G. (Ed.), Compton Scattering, New York, McGraw-Hill, 1977.

3. Cooper M.J., Rep. Progr. Phys., 48, 415 (1985).
4. Jain P.C., Singru R.M. and Gopinathan K.P. (Eds.), Positron Annihilation, Singapore, World Scientific, 1986.
5. Papanicolaou N.I., Bacalis N.C. and Papaconstantopoulos D.A., Phys. Rev. B 37, 8627 (1988).
6. Hedin L. and Lundqvist B.I., J. Phys. C: Solid State Physics, 4, 2064 (1971).
7. Mattheiss L.F., Wood J.H. and Switendick A.C., Methods. Comput. Phys. 8, 63 (1968).
8. Papaconstantopoulos D.A. and Switendick A.C., J. Less Common Met., 103, 317 (1984) and references therein; Papanicolaou N.I., Bacalis N.C. and Papaconstantopoulos D.A., Z. Phys. B: Cond. Matt., 65, 453 (1987).
9. Harthoorn R. and Mijnaerends P.E., J. Phys. F: Met. Phys., 8, 1147 (1978).
10. Gupta M., Solid State Commun. 29, 47 (1979); Phys. Rev. B 25, 1027 (1982).